5th International Conference on Silicon Photovoltaics, SiliconPV 2015

Advanced hydrogenation of dislocation clusters and boron-oxygen defects in silicon solar cells

Brett J. Hallam, Phill G. Hamer, Sisi Wang, Lihui Song, Nitin Nampalli, Malcolm D. Abbott, Catherine E. Chan, Doris Lu, Alison M. Wenham, Ly Mai, Nino Borojevic, Alex Li, Daniel Chen, Moon Yong Kim, Azmeer Azmi, Stuart Wenham

School of Photovoltaics and Renewable Energy Engineering, University of New South Wales, Sydney NSW 2052, Australia

Abstract

Advanced hydrogenation processes targeting the generation of neutrally charged hydrogen (H^0) are applied to passivate structural defects in seeded-cast quasi mono-crystalline silicon wafers and boron-oxygen defects in Czochralski silicon. The application of a one minute laser hydrogenation process onto a finished screen printed solar cell fabricated on the dislocation-rich seeded-cast material resulted in efficiency enhancements of 0.6% absolute through improvements in the implied open circuit voltage and internal quantum efficiency in the vicinity of the dislocated regions. A new insight is presented on the formation of boron-oxygen defects with a strong dependence on illumination intensity. An advanced laser hydrogenation process is presented to rapidly form and hydrogenate boron-oxygen defects simultaneously, in an 8 s process applied directly after belt furnace firing, with the hydrogenation of more than 95% of boron-oxygen defects at a peak temperature of approximately 360 °C on lifetime test structures. The same 8 s process is also demonstrated on standard screen-printed solar cells applied directly after belt furnace firing to simultaneously form- and hydrogenate the boron-oxygen defects, with no subsequent loss in electrical performance, hence avoiding a 0.7% absolute loss in efficiency due to light-induced degradation.

Keywords: defect, hydrogen passivation, hydrogenation, silicon solar cell, regeneration, light induced degradation, boron-oxygen

1. Introduction

1.1. Advanced hydrogen passivation for silicon solar cells

The properties and interactions of hydrogen in silicon have been widely studied over multiple decades. Hydrogen has been shown as highly reactive, with the ability to interact with the silicon lattice and virtually all impurities and

defects within the silicon [1]. Subsequently, hydrogen passivation has been demonstrated to enable substantial improvements to the electrical performance of silicon solar cells through the deactivation of recombination activity associated for a wide array of structural and impurity related defects in silicon solar cells [2].

Hydrogen is a "negative-U" impurity in silicon with the ability to assume different charge states (H^s, where 'S' is the charge state), taking on either a positive (H^+), neutral (H^0) or negative (H^-) charge state [4]. The charge states of the interstitial hydrogen have important implications for both the diffusivity and the ability to interact with defects and impurities within the silicon [5-7]. For example, deep-level monovalent defects in crystalline silicon solar cells including interstitial iron (Fe^+), interstitial chromium (Cr_i^+) and the boron-oxygen (B-O^+) complex are reported to require H^- for defect passivation [8]. However for the case of B-O defects, the actual charge state is unclear. Herring *et al.* have observed that the fractional concentrations of hydrogen $f(H^s)$ depend on the position of the Fermi level in relation to the middle of the forbidden band-gap. Hence, in thermal equilibrium at low temperatures, in p-type silicon, due to a deficiency of free electrons, H^+ is dominant. Similarly in n-type silicon, almost all hydrogen is H^-, and H^0 is always a minority charge species. Therefore, in p-type silicon, the passivation of Fe_i^+, Cr_i^+ and B-O defects by hydrogen would seem unfavorable.

Recent advancements in the understanding of hydrogenation for silicon solar cells have highlighted the importance of using both temperature and carrier injection to manipulate the fractional concentrations of the charge states of the atomic hydrogen and/or the defects within the silicon through the use of temperature and minority carrier injection to improve the effectiveness of hydrogen passivation [7-9]. Two different models have been proposed, one based on the electron quasi-Fermi level [7,9-10], whilst a more complete model based on Sah-Shockley statistics was recently presented by Sun *et al.*, which also considered changes to the fractional charge state concentrations of the defects through modulations in both temperature and excess carrier injection [8]. In both models at low temperatures, increased excess minority carrier concentrations (Δn) results in increased $f(H^-)$. The work by Sun *et al.* also demonstrated that increasing Δn also resulted in an increased product of $f(H^-)$ and the fractional concentration of the defect $f(M)$, where M represents a defect consisting of Fe_i^+, Cr_i^+ or a B-O^+ complex.

1.2. Dislocation clusters in multi-crystalline silicon and seeded-cast quasi mono-crystalline silicon material

Multi-crystalline silicon is prone to a large array of defects such as dislocations, which can occur within the silicon grains, and impurities such as oxygen and metals, which can accumulate at structural defects including grain- and dislocation boundaries [11]. In recent years there have been several approaches proposed for improving the crystalline quality of cast-material, including the development of quasi-mono silicon using the seeded-cast method to grow ingots largely comprising of mono-crystalline silicon [12]. However the quasi mono-crystalline silicon material also suffers from a large variability in crystalline quality. Dislocations may be nucleated by particles and can spread in area throughout the ingot growth due to thermal stresses, potentially covering large portions of a silicon wafer. The dislocations can also induce the growth of multi-crystalline material, particularly around the edge of the ingot [12-13].

The effectiveness of hydrogen passivation for impurity decorated structural defects such as dislocation clusters and grain boundaries has been reported as reduced from that of non-decorated structural defects, with high dislocation densities in the vicinity of grain boundaries also reducing the effectiveness of hydrogen passivation [14]. It has also been reported that the effectiveness of hydrogen passivation at extended crystal defect sites that are already recombination active after crystal growth is also reduced, particularly when decorated with high concentrations of impurities [15]. Hence the passivation of structural defects in cast materials with high dislocation densities such as seeded-cast quasi mono-crystalline silicon appears difficult.

1.3. Permanent mitigation of recombination due to the formation of boron-oxygen defects in Czochralski silicon

The performance of solar cells fabricated using boron-doped Cz silicon is known to degrade under carrier injection due to the formation of a B-O defect [16]. Whilst the degradation can be recovered by thermal annealing in the dark at temperatures greater than 200 °C, subsequent exposure to carrier injection can once again form the B-O defects. In 2006, Herguth *et al.* reported a new approach to prevent lifetime degradation through the use of an illuminated annealing process in which the B-O defect was 'permanently' deactivated, in a process denoted as

'regeneration' [17]. Achieving this state appears to require a fast thermal process (peak temperature over 600 °C) with a high cooling rate followed by a lower temperature illuminated anneal process (generally < 230 °C). However, the exact mechanism of the regeneration process continues to be debated in literature [3,18-22]. Similarly the actual structure of the B-O defect is still a contentious issue, with some groups suggesting the formation of a B-O defect from individual components of boron and oxygen [16], whilst other groups have suggested the transformation of a latent defect complex into a recombination active state [23]. In this paper we use the term defect formation to represent the formation of the recombination active state of defect. Similarly defect dissociation refers to the dissociation of the recombination active defect state back to a recombination inactive state.

Multiple studies from various independent groups have concluded that hydrogen plays a critical role in the permanent deactivation of boron-oxygen B-O complexes [3,18-21]. It has been noted that hydrogen-free dielectric layers deposited by low-pressure chemical vapour deposition and do not enable the regeneration process, and that it requires a dielectric layer containing hydrogen such as plasma-enhanced chemical vapour deposited (PECVD) silicon nitride [3]. Hydrogen content has also been shown to change the rate and effectiveness of the hydrogenation process by multiple authors [18-19]. Influences of plasma processing on hydrogen diffusivity have also been suggested as a likely mechanism [24]. In addition, some studies have reported a lack of regeneration when wafers are fired in the absence of a hydrogen-containing film prior to the illuminated annealing process [3,18-19]. This suggests that the influence of firing is not purely thermal. However, direct comparison between bare-fired wafers and those fired with hydrogen-containing dielectrics or even with different dielectric layers has been difficult due to the differing levels of surface passivation and the consequent impact on lifetime and open circuit voltage, casting uncertainty on whether regeneration is truly possible without the presence of hydrogen during firing, or whether the process is actually enabled by a plasma process prior to firing. It has also been hypothesized that the charge state of hydrogen could play a key role in the passivation process for B-O defects [8,20,25].

Despite all of the evidence suggesting the involvement of hydrogen, an alternative theory based on a purely thermal mechanism was proposed by Walter *et al.*, involving the formation of boron nano-precipitates during fast firing, suggesting that hydrogen was in no way involved in the regeneration process [22]. However, the understanding of the proposed hydrogen-free mechanism for B-O regeneration in that work were developed based on data from wafers with hydrogen containing dielectric layers.

Traditionally this permanent deactivation processes has taken 2 hours to complete, a timeframe not compatible with inline processing. Therefore, the development of rapid processes has become an area of recent interest. Rapid processes to hydrogenate B-O defects have been demonstrated by Wilking *et al.* on non-diffused lifetime test structures with complete passivation of the B-O defects in approximately 10 s at 230 °C under 2.7 suns illumination. This result has highlighted the potential for the B-O defect to be passivated in an in-line environment [21]. A further acceleration of the defect passivation process was presented using localised laser-induced hydrogenation with time constants under laser exposure of less than 1 s [26]. The authors highlighted the negative influence of emitters in slowing down the regeneration process, which would therefore reduce the regeneration rate for finished solar cells. In both studies test structures typically started in a degraded state (i.e. with the defects fully formed after a 24 h or 48 h light soaking process) as opposed to the state of the wafers would be in immediately after the last solar cell processing step (i.e. no B-O defects present). On cells, a number of authors have reported times to permanently deactivate B-O defects of approximately 2 hours, although this can be reduced to 10 – 30 minutes at temperatures approaching 200 °C [27-28]. In some instances, this time also includes defect formation.

In this paper, we explore the use of high intensity illumination for the passivation of dislocation clusters in seeded-cast quasi mono-crystalline silicon and B-O defects in boron-doped Cz silicon. We also aim to conclusively show that the presence of hydrogen during fast firing is essential to enable the permanent deactivation process, and that it is not a purely thermal based mechanism, or solely due to exposure to a plasma exposure prior to fast firing. We will also demonstrate a rapid 8 s process to hydrogenate boron-doped Cz silicon based on a new and improved understanding of both B-O defect formation and hydrogenation, with simultaneous defect formation and hydrogenation that can be applied directly after belt furnace firing.

2. Experimental details

2.1. Fabrication of- and laser hydrogenation of screen-printed solar cells

In this paper, standard screen printed solar cells were fabricated on commercial grade 156 mm × 156 mm wafers comprising of both 1 Ωcm boron-doped seeded-cast quasi mono-crystalline silicon wafers and 1.6 Ωcm boron-doped Cz silicon. Wafers were alkaline textured with a resultant thickness of approximately 180 μm. Wafers were subjected to an RCA clean and HF dip, followed by phosphorus emitter formation in a POCl$_3$ tube furnace to a sheet resistance of ~70 Ω/sq. After phosphosilicate glass (PSG) removal, hydrogenated silicon nitride (SiN$_x$:H) with a refractive index of 2.08 at 633 nm and thickness of 75 nm was deposited onto the front surface of the wafer using a Roth & Rau MAiA PECVD system. Prior to screen printing, solar wafers were cleaved into 16 pieces to aid with subsequent laboratory processing. A full area Al back surface field and front Ag contacts were formed by screen printing and subsequent firing in an in-line SierraTherm belt furnace. Firing was performed as per the paste manufacturers' recommendations.

Laser hydrogenation was performed on the finished solar cells with no intermediate thermal or illumination processes to modulate defect formation (i.e. form B-O defects). The laser hydrogenation system comprised a high-powered laser with a hot plate to modulate both temperature and carrier injection.

2.2. Investigating the role of hydrogen in the mitigation of boron-oxygen related degradation

To investigate the role of hydrogen in the 'regeneration' process, symmetrical lifetime test structures were prepared using the same source of boron-doped Cz wafers as mentioned above. After alkaline texturing, an emitter diffusion was performed to a sheet resistance of ~200 Ω/sq to aid in surface passivation. The resulting PSG was removed in dilute HF and wafers were divided into four groups for further processing:

- (A) The first group did not receive SiN$_x$:H layers during the first round of SiN$_x$:H depositions (SiN$_x$:H Deposition 1), and were not fired.
- (B) The second group underwent rapid thermal processing (firing) bare (with no prior exposure to SiN$_x$:H deposition), i.e. no hydrogen source was present on the wafer during firing.
- (C) The third group had initial layers of SiN$_x$:H deposited on both sides (SiN$_x$:H Deposition 1) but was not fired. i.e. No thermal process was performed after the deposition of SiN$_x$:H.
- (D) The fourth group had initial layers of SiN$_x$:H deposited on both sides (SiN$_x$:H Deposition 1) and were fired.

The SiN$_x$:H layers in groups C and D were etched after firing (5 % HF for 10 min). A second SiN$_x$:H deposition was then performed for all wafers (SiN$_x$:H Deposition 2) to eliminate differences in surface passivation that could result from firing wafers with and without the initial SiN$_x$:H films. All SiN$_x$:H layers were identical to the layers deposited in the first SiNx:H deposition. On a further group, SiN$_x$:H was deposited onto the wafer, but removed prior to firing to directly compare any influence of the plasma process with firing from the requirement to have the SiN$_x$:H layer present during firing.

Firing was performed in a SierraTherm infra-red fast-firing furnace. Thermal profiling performed using a Datapaq Q18 profiler confirmed that samples with and without the SiN$_x$:H films underwent the same thermal process. A peak temperature of 600 °C was achieved and a belt speed of 5.0 m/min was used, resulting in a rapid cooling rate of 50 ± 1 °C/s between 600 °C and 550 °C. In specific instances the peak firing temperature was altered from 450 °C up to 800 °C in the presence of SiN$_x$:H layers during firing.

Wafers in all groups were then subjected to an initial light-induced degradation (LID-1) process as described below in Section 2.5. An illuminated annealing step was then performed for 2 hours at 172 ± 3 °C under a halogen lamp with a light intensity of 65 ± 2 mW/cm^2. A second and final degradation step (LID-2) was then performed under the same conditions as LID-1. In all cases, the duration of the LID process was found to be sufficient to completely degrade sample lifetimes.

2.3. Fabrication of lifetime test structures for a rapid formation of- and rapid hydrogenation of B-O defects

Symmetrical lifetime test structures were fabricated as described in Section 2.2 above, with all wafers receiving identical SiN$_x$:H layers. To purely investigate degradation kinetics without the introduction of hydrogen, samples were not fired. For investigations on rapid hydrogenation of B-O defects, wafers were fired as described above with a peak firing temperature of approximately 600 °C. Both degradation and hydrogenation were performed with the same laser system as described above. For lifetime test structures investigating the rapid hydrogenation of B-O defects, samples were prepared both with and without a dark annealing process performed directly after belt furnace firing. Monitoring of the wafer temperature was performed using a DataPaq Q18 thermal profiler.

2.4. Characterisation methods

To characterize the impact of B-O defects, the bulk lifetime (τ_{bulk}) of each sample was measured after each of the processing steps. This was done by measuring the effective minority carrier lifetime (τ_{eff}) as a function of Δn using a WCT-120 (Sinton Instruments) photoconductance lifetime tester with nine points sampled per wafer [29]. The measured data was analysed using the generalised method [30] and corrected for Auger recombination [31]. To enable a comparison between the different groups, and remove the impact of variations in surface recombination, a value for τ_{bulk} was extracted at a carrier concentration of 2×10^{14} /cm^3. This was done by assuming the surfaces were well modelled by the dark saturation current density (J_{0d}) values, which were extracted from the slope of the original lifetime curve at $\Delta n = 1 \times 10^{16}$ /cm^3 directly after the second SiN$_x$:H deposition, hence prior to the introduction of Shockley-Read-Hall (SRH) recombination during LID-1. Note that the resulting τ_{bulk} included the contribution of Shockley-Read-Hall (SRH) defect recombination [32]. For samples significantly affected by bulk asymmetric SRH recombination (for steps LID-1, the illuminated anneal and LID-2), the extraction of J_{0d} resulted in values that were slightly underestimated, causing a slight overestimation of τ_{bulk}, but do not affect the trends or conclusions drawn.

Current density-voltage (J-V) measurements were performed on the finished solar cells, after laser hydrogenation and after stability testing. Light beam-induced current (LBIC) measurements were performed on the seeded-cast solar cells before and after laser hydrogenation.

2.5. Stability testing for B-O defects

A light-induced degradation (LID) process for stability testing was performed on relevant lifetime samples and solar cells under a halogen lamp with a light intensity of 78 ± 1 mW/cm^2 at a temperature of 40 ± 3 °C for a total of 48 hours. In all cases, the duration of the LID process was sufficient to completely degrade sample lifetimes.

Where relevant, dark annealing was performed on all lifetime samples on a hot plate with a wafer temperature of approximately 230 °C for 10 min to thermally dissociate B-O defects.

3. Results and discussion

3.1. Laser-enhanced hydrogenation of dislocation clusters

The solar cells displayed a strong reduction in internal quantum efficiency (IQE) at 981 nm in the vicinity of dislocation clusters (Fig. 1a). After a 1 minute laser hydrogenation process at approximately 430 °C under 80 suns of illumination, substantial improvements in IQE were observed in such regions (Fig. 1b). Furthermore, an enhancement in IQE at 404 nm was observed over the entire cell area (not shown). Subsequently, the efficiency of the solar cell increased by 0.6 % absolute (Fig. 1c), with large improvements in short circuit current density (J_{SC}) and open circuit voltage (V_{OC}). Further details on this process have been presented by Song *et al.* [33].

The increased IQE in the dislocated regions of the solar cell suggest a reduction in recombination activity was achieved in the vicinity of these regions through the laser hydrogenation process. It appears that the defect may be passivated by H^0 as it falls within theoretically predicted regions to greatly increase f(H^0) [10]. Furthermore, the ineffectiveness of conventional hydrogenation processes performed during fast-firing for screen-printed contact formation is highlighted, whereby a short subsequent advanced hydrogenation process lead to substantial efficiency

enhancements. In addition, the improved passivation was stable under exposure to further illumination and/or thermal treatments.
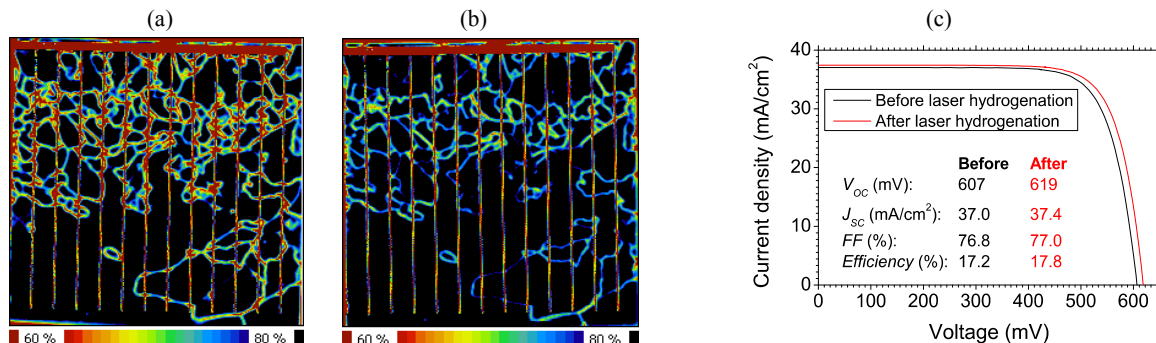

Fig. 1. LBIC images at 981 nm of a screen-printed solar cell fabricated on seeded-cast quasi mono-crystalline silicon (a) before and (b) after laser hydrogenation. (c) J-V curve of the corresponding cell.

3.2. The necessity of hydrogen to mitigate boron-oxygen related degradation

The influence of the SiN_x:H layers and rapid thermal processing on the sample lifetime, shown in Fig. 2, demonstrate experimentally the involvement of hydrogen in the permanent deactivation process. The τ_{bulk} of the various groups as well as the J_{0d} were primarily unaffected by prior processing. Hence prior firing, or prior SiN_x:H deposition did not influence the surface passivation after SiN_x:H Deposition 2. After the first LID process (LID-1), the τ_{bulk} of all groups was reduced. After the illuminated annealing process, only samples fired with SiN_x:H present showed a substantial recovery of the carrier lifetime, which was also stable under subsequent 1-sun illumination. Hence samples fired under identical thermal conditions in the absence of the SiN_x:H layer did not see this recovery in carrier lifetime.
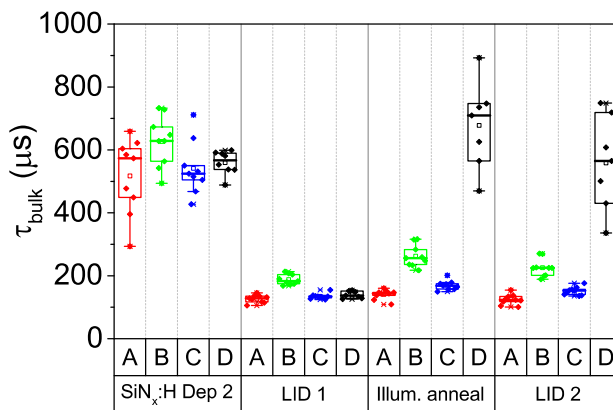

Fig. 2. Bulk minority carrier lifetimes (τ_{bulk}) extracted at an excess carrier density of $\Delta n = 2 \times 10^{14}$ /cm^3 after various processes including a second round of SiN_x:H depositions (SiN_x:H Dep 2), light induced degradation (LID-1), illuminated annealing (Illum. anneal) and subsequent stability testing (LID-2). Groups consist of: (A) – no SiN_x:H deposition 1, not fired, (B) – no SiN_x:H deposition 1, fired, (C) – with SiN_x:H deposition 1, not fired, and (D) – with SiN_x:H deposition 1, fired.

The results based on prior exposure to plasma without firing for group C (SiN_x:H deposition 1 or 2), as well as A and B (for SiN_x:H deposition 2) and subsequent processing, indicated that the stable recovery was not purely related to prior exposure to a plasma. However conclusions of the influence of exposure to plasma in conjunction with a firing process on τ_{bulk} cannot be drawn from these results. Further insight into the influence of prior exposure to a

plasma in conjunction with firing was provided by an additional group in which an initial SiN_x:H layer was deposited onto the sample, but removed prior to firing. On this sample, no recovery was observed, and hence the permanent recovery process is not simply due to an interaction of prior plasma exposure in conjunction with firing. Hence in this work a SiN_x:H layer was required to be deposited, and the wafer required to be fired with the SiN_x:H present, to enable the permanent recovery of the lifetime, giving further evidence for the importance of hydrogen in this process. Further details are shown in [34].

This implies that the influence of firing to enable the 'regeneration' process was not purely thermal. Furthermore, a partial but stable recovery of lifetime could be achieved with actual peak firing temperatures on the wafer as low as 450 °C, and full recovery could be achieved for peak firing temperatures > 500 °C, well below that being reported as critical in the thermally based theory with boron nano-precipitate formation [22]. Further details of this low temperature activation for subsequent recovery will be presented elsewhere. It is expected that the low temperatures used in this work to enable this stable recovery of the carrier lifetime associated with B-O related degradation was due to a number of factors. Firstly, the release of hydrogen from the SiN_x:H layer is affected by the SiN_x:H film composition. That is, the composition of the layer will affect the temperature at which effective hydrogen release can be realised at, independently of the hydrogen content of the film. Secondly, the ability of hydrogen to diffuse into the silicon is affected by temperature, the solar cell structure (i.e. the presence of hydrogen diffusion blocking layers such as dielectric layers and diffused layers), and the charge state of the hydrogen during the firing process [25].

The results in this section highlight that such a method could be used to evaluate the role of hydrogen in defect passivation for a range of defects, provided that the second SiN_x:H deposition does not thermally dissociate the hydrogen-defect complex of interest, or that the targeted hydrogenation process is applied after the second SiN_x:H deposition (as is the case for B-O defects in this work), where the firing is merely to incorporate hydrogen into the bulk of the silicon.

3.3. Rapid formation of B-O Defects in Czochralski silicon

The formation of B-O defects in boron-doped Cz silicon is greatly dependent on the illumination intensity provided. Fig. 3 shows curves of Auger corrected inverse effective minority carrier lifetime ($1/\tau_{eff} - 1/\tau_{Aug}$) as a function of Δn of non-fired samples. Curves are shown directly after SiN_x:H deposition (before exposure to laser illumination), after 1 min of exposure to laser illumination (938 nm) at 150 °C with an illumination intensity of either 1-sun or 80-sun, after dark annealing and after a subsequent stability test with 48 h of illumination. Complete degradation was observed for the sample with 80 suns (1.68×10^{19} photons/cm^2/s) illumination during the degradation process, whilst only a partial degradation was observed for the sample under 1 sun (2.1×10^{17} photons/cm^2/s) illumination. Further acceleration of the defect formation can be achieved using increases in the temperature and/or illumination intensity, with near complete defect formation demonstrated in less than 4 seconds [35]. In comparison, using a characteristic frequency for defect formation of 1×10^{3} /s, consistent with a recent degradation study [36], under low injection conditions, in 4 seconds less than 10% of defects would form using an identical thermal profile [35].

The results suggest a dependence on the total hole density rather than the equilibrium hole concentration as reported in the literature [36-38]. Hence these results are in contradiction with many authors findings that the formation rate beyond very low illumination intensities (0.01 sun), is independent of illumination intensity [39-40]. However these results are in agreement with a speculation by Macdonald *et al.* that excess holes may play a role [37]. In previous work, low illumination intensities were used of up to 2 suns, and hence illumination intensities over 0.1 suns only reflect the saturation of the process requiring minority carriers, rather than an influence of majority carriers as were used in this work. In this work, the high illuminations used allow a temporary, but substantial increase in total hole concentration to accelerate the defect formation process. With this new and improved insight, carrier lifetimes and the solar cell structure can therefore influence the defect formation rate. Further information on this understanding is provided in [35].

We believe that the rapid formation of B-O defects is critical to allow a rapid hydrogenation of B-O defects in boron-doped Cz material, as it allows the B-O defects to be available for hydrogenation sooner, in instances where the defect formation rate may itself limit the rate at which the B-O defects can be hydrogenated. Furthermore, the

rapid formation of B-O defects can allow a rapid re-formation of thermally dissociated B-O defects at elevated temperatures due to the acceleration of the thermal dissociation process during the hydrogenation process.
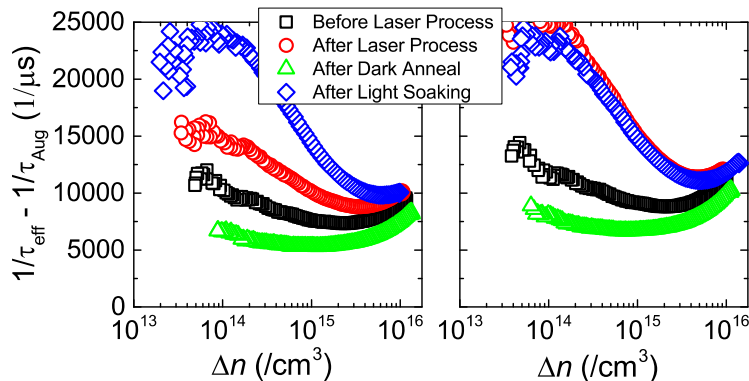

Fig. 3. Auger corrected inverse effective minority carrier lifetime ($1/\tau_{eff}$ - $1/\tau_{Aug}$) as a function of minority carrier density (Δn) for samples with laser degradation performed at 150 °C for 1 min, for (left) 1 sun illumination showing partial degradation and (right) 80 suns illumination showing complete degradation.

3.4. Rapid laser hydrogenation of B-O defects in Czochralski silicon solar cells

Boron-doped Cz silicon can be fully hydrogenated within seconds including defect formation. Fig. 4 shows Auger corrected inverse effective minority carrier lifetime curves as a function of Δn on fired samples. Curves are shown after belt furnace firing and a subsequent dark anneal, after laser hydrogenation (8 s under 160 sun illumination with a peak temperature of 360 °C to generate H^0) and after subsequent light soaking (green squares) with only a slight increase in inverse effectively minority carrier lifetime. For comparison a curve is also shown of a similarly processed sample that did not receive the laser hydrogenation treatment (blue triangles) and hence degraded during the light soaking process. The effectiveness of the process was approximately 95%, whilst other processes up to the same temperature have shown an improved effectiveness in excess of 98%. This demonstrates that effective hydrogenation of B-O defects can be improved at temperatures above 230 °C by increasing the illumination intensity, when compared to previous work using an illumination intensity of 2.7 suns [26]. In this work, the improved hydrogenation is attributed to accelerated defect formation [35].
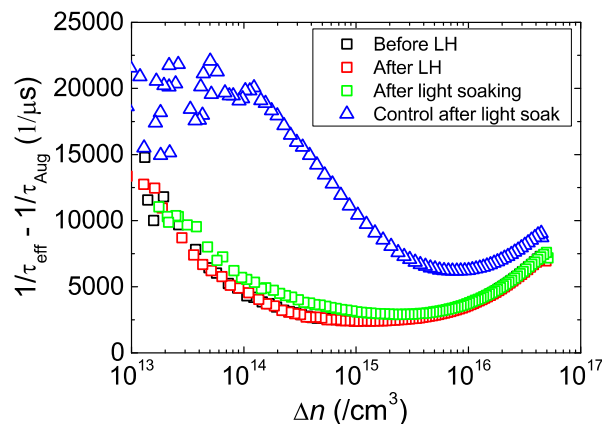

Fig. 4. Auger corrected inverse effective minority carrier lifetime ($1/\tau_{eff}$ - $1/\tau_{Aug}$) as a function of minority carrier density (Δn) for samples after firing and a dark anneal (before laser hydrogenation (LH)), after an 8 s laser hydrogenation process with a peak temperature of 360 °C at an illumination intensity of 160 suns, after light soaking for 48 hours (green squares). As a comparison, a curve is shown after light soaking of a sample that did not receive the laser hydrogenation treatment (blue triangles) highlighting the expected lifetime degradation in the material without hydrogenation of the B-O defects.

It should be noted that identical results were obtained on samples without a dark annealing process applied directly after belt furnace firing. Hence the dark anneal had no influence on the ability to rapidly hydrogenate the B-O defects. It is expected that the time required to achieve effective hydrogenation was limited by the experimental setup due to the time taken to heat the sample under laser illumination. Using processing times as short as 2 s have resulted in the hydrogenation of approximately 90% of boron-oxygen defects in the material (not shown).

The same 8 s laser hydrogenation process was applied to finished screen printed solar cells directly after belt furnace firing, that is, with no intermediate thermal or illumination processes to modulate the state of boron and oxygen in the wafer. No loss in electrical performance was observed after subsequent stability testing on laser-hydrogenated samples. As a comparison, a cell that did not receive the laser hydrogenation process degraded by 0.7% absolute from the value obtained at the end of cell fabrication process, after the subsequent stability test (48 h). Hence the 8 s laser hydrogenation process completely mitigated any significant performance loss due to the formation of B-O defects. Further details of the rapid hydrogenation process will be published elsewhere.

Table 1. One-sun stabilised J-V data for screen-printed solar cells fabricated on standard commercial grade 1.6 Ωcm boron-doped wafers. Results are shown for a solar cell that received an 8 s laser hydrogenation process directly after belt furnace firing (with 160 sun illumination intensity and a peak temperature of 360 °C), and for a control that did not receive the laser hydrogenation treatment.

Stage of Processing	V_{OC} (mV)	J_{SC} (mA/cm^2)	FF (%)	Efficiency (%)
Laser hydrogenated	631.6	37.3	78.8	18.6
Control	620.4	36.7	78.6	17.9

4. Conclusions

In this paper, an advanced laser hydrogenation process was applied to finished screen-printed solar cells fabricated on dislocation-rich seeded-cast quasi mono-crystalline silicon. The application of the laser hydrogenation process with high intensity illumination to target the generation of H^0 resulted in an increase in cell efficiency of 0.6% absolute, with large increases in the V_{OC} and J_{SC} of the device. The IQE at 981 nm greatly improved in the in the dislocated regions, indicating an improved effectiveness of the hydrogenation of the structural defects.

A study was also conducted to separate thermal effects during fast-firing from hydrogen and plasma related effects in modulating the B-O defect. It was concluded that the influence of fast-firing was not purely thermal, and that a hydrogen containing dielectric layer (in this work SiN_x:H) was required to be present during fast firing to enable the permanent recovery of carrier lifetimes associated with the formation of the B-O defect. Furthermore, the process was not purely due to plasma exposure prior to firing, and that the lifetime recovery could be activated by a firing process with a peak temperature as low as 450 °C.

A process was demonstrated to enhance the defect formation rate of B-O defects using high intensity illumination, based on a new understanding where the defect formation rate is dependent on the total hole concentration rather than the equilibrium hole concentration. Full defect formation could be achieved within 4 s, and noted as an essential precursor for the hydrogenation of B-O defects. Subsequently, rapid hydrogenation of B-O defects was demonstrated with an 8 s process applied directly after belt furnace firing to both form and hydrogenate more than 95% of the B-O defects at a peak temperature of 360 °C. This process used high intensity illumination to accelerate defect formation and simultaneously target the formation of H^0. The process was also demonstrated on screen-printed solar cells, with no subsequent loss of efficiency. In compassion, solar cells that did not receive the laser hydrogenation process suffered a 0.7% absolute reduction in efficiency due to the light-induced degradation.

Acknowledgements

Institution of Engineering and Technology (IET) for their funding support for this work through the A.F. Harvey Engineering Prize.

References

[1] Sopori B. Silicon solar-cell processing for minimizing the influence of impurities and defects. J. of Elec. Mat. 2002;31(10):972–980.

[2] Karzel P, Junge J, Hahn G. Mapping of hydrogen bond energies in EFG silicon samples by analysis of spatially resolved minority charge carrier lifetimes after annealing steps. Proc. of the 24th European Photovoltaic Solar Energy Conference, Hamburg. 2009;2023–2027.

[3] Münzer K. Hydrogenated Silicon Nitride for Regeneration of Light Induced Degradation. Proc. 24th EU PVSEC, Hamburg. 2009;1558–61.

[4] Herring C, Johnson N, Van de Walle CG. Energy levels of isolated interstitial hydrogen in silicon. Physical Review B. 2001;64(12):125209.

[5] Mathiot D. Modeling of hydrogen diffusion in n-and p-type silicon. Physical Review B. 1989;40(8):5867–5870.

[6] Johnson N, Herring C, Chadi D. Interstitial hydrogen and neutralization of shallow-donor impurities in single-crystal silicon. Phys. Rev. Lett. 1986;56(7):769–72.

[7] Hallam BJ, Hamer PG, Wenham SR, Abbott MD, Sugianto A, Wenham AM, Chan CE, Xu QX, Kraiem J, Degoulange J, Einhaus R. Advanced Bulk Defect Passivation for Silicon Solar Cells. IEEE Journal of Photovoltaics. 2014 Jan;4(1):88–95.

[8] Sun C, Rougieux FE, Macdonald D. A unified approach to modelling the charge state of monatomic hydrogen and other defects in crystalline silicon. Journal of Applied Physics. 2015;117(4):045702.

[9] Hamer P, Hallam B, Wenham S, Abbott M. Manipulation of Hydrogen Charge States for Passivation of p-type Wafers in Photovoltaics. IEEE Journal of Photovoltaics. 2014;4(5):1252–1260.

[10] Hamer P, Hallam B, Chan C, Wenham A, Sugianto A, Abbott M, Wenham S. Hydrogen passivation mechanisms in silicon solar cells. Proc. 28th European PVSEC, Paris, France. 2013;p. 982–987.

[11] Schultz O, Glunz S, Riepe S, Willeke G. High-efficiency solar cells on phosphorus gettered multicrystalline silicon substrates. Progress in Photovoltaics: Research and Applications. 2006;14(8):711–719.

[12] Stoddard N, Wu B, Witting I, Wagener MC, Park Y, Rozgonyi GA, George A, Clark R. Casting single crystal silicon: novel defect profiles from BP Solar's mono2 TM wafers. Solid State Phenomena. 2008;131:1–8.

[13] Gu X, Yu X, Guo K, Chen L, Wang D, Yang D. Seed-assisted cast quasi-single crystalline silicon for photovoltaic application: Towards high efficiency and low cost silicon solar cells. Solar Energy Materials and Solar Cells. 2012;101:95–101.

[14] Chen J, Sekiguchi T. Carrier recombination activity and structural properties of small-angle grain boundaries in multicrystalline silicon. Japanese Journal of Applied Physics. 2007;46(10R):6489.

[15] Geerligs L, Komatsu Y, Röver I, Wambach K, Yamaga I, Saitoh T. Hydrogen passivation of iron in multicrystalline silicon. Journal of Applied Physics. 2007;102(9):093702.

[16] Schmidt J, Aberle AG, Hezel R. Investigation of carrier lifetime instabilities in Cz-grown silicon. Proc. 26th IEEE PVSC. 1997;p. 13–18.

[17] Herguth A, Schubert G, Käs M, Hahn G. A new approach to prevent the negative impact of the metastable defect in boron doped Cz silicon solar cells. Proc. of the 4th IEEE World Conference on Photovoltaic Energy Conversion. 2006;1:940–943.

[18] Krugel G, Wolke W, Geilker J, Rein S, Preu R. Impact of Hydrogen Concentration on the Regeneration of Light Induced Degradation. Energy Procedia. 2011;8:47–51.

[19] Dubois S, Tanay F, Veirman J, Enjalbert N, Stendera J, Butté S, . The BOLID Project: Suppression of the Boron-Oxygen Related Light-Induced-Degradation. Proc. 27th European PVSEC, Frankfurt, Germany. 2012;p. 749–754.

[20] Hallam B, Wenham S, Hamer P, Abbott M, Sugianto A, Chan C, Wenham A, Eadie M, Xu, G. Hydrogen passivation of B-O defects in Czochralski silicon. Energy Procedia. 2013;38:561–570.

[21] Wilking S, Beckh C, Ebert S, Herguth A, Hahn G. Influence of bound hydrogen states on BO-regeneration kinetics and consequences for high-speed regeneration processe. Solar Energy Materials and Solar Cells. 2014;131:2–8.

[22] Walter D, Lim B, Bothe K, Voronkov V, Falster R, Schmidt J. Effect of rapid thermal annealing on recombination centres in boron-doped Czochralski-grown silicon. Applied Physics Letters. 2014;104(4):042111.

[23] Voronkov, Vladimir V and Falster, R. Latent complexes of interstitial boron and oxygen dimers as a reason for degradation of silicon-based solar cells. Journal of Applied Physics. 2014;110(6):063515.

[24] Lim B, Bothe K, Schmidt J. Accelerated deactivation of the boron-oxygen-related recombination centre in crystalline silicon. Semiconductor Science and Technology. 2011;26(9):095009.

[25] Wenham S, Hamer P, Hallam B, Sugianto A, Chan C, Song L, Lu PH, Wenham AM, Mai L, Chong CM, and Xu GX, and Edwards MB. Advanced hydrogenation of silicon solar cells; 2013. WO2013173867 A1.

[26] Wilking S, Engelhardt J, Ebert S, Beckh C, Herguth A, Hahn G. High Speed Regeneration of BO-Defects: Improving Long-Term Solar Cell Performance within Seconds. Proc. 29th European PVSEC. 2014:366–372.

[27] Herguth A, Hahn G. Kinetics of the boron-oxygen related defect in theory and experiment. J. of Applied Physics. 2010;108(11):114509.

[28] Lim B, Hermann S, Bothe K, Schmidt J, Brendel R. Deactivation of the boron-oxygen recombination center in silicon by illumination at elevated temperature. Applied Physics Letters. 2008;93(16):162102–162102.

[29] Sinton RA, Cuevas A, Stuckings M. Quasi-steady-state photoconductance, a new method for solar cell material and device characterization. Proceedings of the 25th IEEE Photovoltaic Specialists Conference. 1996;p. 457–460.

[30] Nagel H, Berge C, Aberle AG. Generalized analysis of quasi-steady-state and quasi-transient measurements of carrier lifetimes in semiconductors. Journal of Applied Physics. 1999;86(11):6218–6221.

[31] Richter A, Werner F, Cuevas A, Schmidt J, Glunz S. Improved parameterization of auger recombination in silicon. Energy Procedia. 2012;27:88–94.

[32] Macdonald D, Cuevas A. Validity of simplified Shockley-Read-Hall statistics for modeling carrier lifetimes in crystalline silicon. Physical Review B. 2003;67(7):075203.

[33] Song L, Wenham A, Wang S, Hamer P, Shakil A, Hallam B, Mai L, Abbott M, Hawkes E, Chong C, Wenham S. Laser enhanced hydrogen passivation of silicon wafers. International Journal of Photoenergy. 2015;501:193892.

[34] Nampalli N, Hallam B, Chan C, Abbott M, Wenham S. Evidence for the role of hydrogen in the stabilization of minority carrier lifetime in boron-doped Czochralski silicon. Applied Physics Letters. 2015;106(17):173501.

[35] Hamer P, Hallam B, Wenham S, Abbott M. Accelerated Formation of the Boron-Oxygen Complex in p-type Czochralski Silicon. Physica status solidi: Rapid research letters. 2015; http://dx.doi.org/10.1002/pssr.201510064.

[36] Nærland TU, Haug H, Angelskar H, Sondena R, Marstein ES, Arnberg L. Studying Light-Induced Degradation by Lifetime Decay Analysis: Excellent Fit to Solution of Simple Second-Order Rate Equation. Photovoltaics, IEEE Journal of. 2013;3(4):1265–1270.

[37] Macdonald D, Liu A, Cuevas A, Lim B, Schmidt J. The impact of dopant compensation on the boron-oxygen defect in p-and n-type crystalline silicon. Physica status solidi (a). 2011;208(3):559–563.

[38] Lim B, Rougieux F, Macdonald D, Bothe K, Schmidt J. Impact of oxygen on the permanent deactivation of boron--oxygen-related recombination centers in crystalline silicon. Journal of Applied Physics. 2010;108:103722.

[39] Schmidt J, Bothe K. Structure and transformation of the metastable boron- and oxygen-related defect center in crystalline silicon. Physics Review B. 2004;69:024107.

[40] Nærland TU, Angelskår H, Marstein ES. Direct monitoring of minority carrier density during light induced degradation in Czochralski silicon by photoluminescence imaging. Journal of Applied Physics. 2013;113(19):193707.